

Synchronization of femtosecond laser and electron pulses with subpicosecond precision

H. Park, Z. Hao, X. Wang, S. Nie, R. Clinite, and J. Cao^{a)}

Physics Department and National High Magnetic Field Laboratory, Florida State University, Tallahassee, Florida 32310

(Received 11 April 2005; accepted 13 June 2005; published online 22 July 2005)

The temporal evolution of electron shadow images, formed by the projection of primary femtosecond electron pulses (probe) over a metal target and perturbed by the transient space-charge field near the target surface induced by the excitation of femtosecond optical pulses (pump), is recorded in real time. By quantitatively analyzing the evolution of these shadow images as a function of pump-probe delay times, we are able to synchronize the femtosecond laser and electron pulses with sub-ps precision. This approach is independent of the structural dynamics under investigation and can be applied to a variety of diffraction setups and target materials using laser pulses of different wavelengths. © 2005 American Institute of Physics. [DOI: 10.1063/1.1994922]

I. INTRODUCTION

Recent advances in time-resolved electron diffraction have provided the capability of direct measurement of ultrafast structural changes on the picosecond (ps) and sub-ps time scale.^{1–9} In particular, taking advantage of the very strong electron-atom scattering, a diffraction pattern recorded with a single femtosecond (fs) pulse containing only a few thousand electrons has been demonstrated to have sufficient signal-to-noise ratio (SNR) for the investigation of nonreversible order-disorder structural phase transitions in solids on the sub-ps time scale.⁶ Very recently, femtosecond electron diffraction (FED) has been used to monitor the laser-induced lattice dynamics in thin film aluminum in the relatively low excitation region where temporal evolution of both coherent and thermal lattice motions was directly measured in real time.^{10,11}

Despite these rapid progresses, one of the most critical issues is that the synchronization of the femtosecond excitation laser (pump) and probe electron pulses in the interaction region on the sub-ps time scale, remains unresolved. Apparently, accurate determination of this time zero point is crucial for the study of nonreversible structural dynamics such as laser-induced melting of thin films. In these types of experiments, laser-induced sample damage limits the total number of available diffraction patterns and prevents the extensive search for time zero. In the cases where sample damage is less crucial, such as reversible structural changes in solids and photoreactions in gas phase, time zero can be, in principle, extracted from the temporal evolution of structural changes under investigation. Nonetheless, the independent and accurate determination of time zero will undoubtedly help narrow down the scan range and ultimately result in higher SNR for more accurate structure determination in a given experimental time span. This is particularly true for

gas-phase diffraction, since each data point requires at least a few hours integration time due to the weak diffraction signal associated with the lack of long-range order.

In this article, we report on an independent means for determining the time zero point in time-resolved electron diffraction with sub-ps precision, irrespective of the structural dynamics under investigation. The principle of this approach should be applicable to a variety of diffraction setups, including cross-beam gas phase and transmission diffraction for solids, different target geometry and materials, and laser excitation pulses of different wavelengths.

II. METHODOLOGY

In contrast to the all-optical time-resolved experiments, the accurate determination of time zero point with sub-ps accuracy in time-resolved electron diffraction is by no means trivial. In principle, approaches based upon the direct interactions of electrons with photons, such as pondermotive scattering,^{12–14} Thomson scattering,¹⁵ second harmonic generation,¹⁶ and Kapitza–Dirac scattering,^{17,18} can provide an exact cross correlation for accurate time zero measurement. However, they require either very high density of electrons and photons in the interaction region, or special setups not inherent to a typical time-resolved diffraction experiment. In practice, these approaches are further constrained by extremely small electron numbers, since in most cases the average number of electrons is limited to a few thousand per pulse by the space-charge effect. Among the above direct approaches, pondermotive scattering holds the potential to produce readily detectable deflection of the incident electron beam. Nevertheless, its effectiveness and feasibility for the stringent sub-ps electron diffraction conditions, such as extremely low electron number and 30–60 keV high beam energy, remains to be experimentally verified.

An alternative approach of finding time zero is to monitor the dynamics of electron-photon interactions via an intermediary. Similar approaches have been used routinely for finding time zero in femtosecond all optical pump-probe ex-

^{a)} Author to whom correspondence should be addressed; electronic mail: jcao@magnet.fsu.edu

periments, such as using the photoexcited transient states in molecules as an intermediary.¹⁹ Along this line, a pair of streaking plates was installed at the sample position in the first ps electron diffraction study of laser melting of thin aluminum films²⁰ and was used to generate a transient electric field following the activation of a GaAs photoconductive switch by laser pulses. By recording the correlation between the electron beam deflection and the timing of switching the laser pulse, time zero was determined to within 5–10 ps.

Another elegant example of this indirect approach was the photoionization-induced lensing (PIL) in gas-phase ultrafast diffraction,²¹ which was conducted with a nearly identical experimental setup. In PIL, the nascent photoelectrons generated by multiphoton ionization of gas molecules escape the ionization region, leaving behind a cylindrical column of positively charged ions along the pump laser path. The transient electric field associated with this newly formed plasma acts as an effective lens and induces change in the electron beam shape. By monitoring the corresponding electron beam profile change, the time zero was determined with a few ps accuracy, which is limited primarily by the relatively slow buildup time of the positive plasma field. Later, the accuracy of this PIL was improved to near 1 ps by intentionally letting the excitation laser beam clip the stainless-steel gas nozzle tip.^{1,22} It appears that this coexcitation of the gas and the nozzle tip somehow accelerated the buildup of transient positive electric field near the tip, which facilitated a more accurate determination of time zero.

The method of synchronization presented here is also based on the real time imaging of the profile change of an electron beam via its interaction with an intermediary: a transient space-charge field resulting from the laser excitation of a metal surface in a high or ultrahigh vacuum. Following intense fs laser excitation, the majority of low energy electrons ejected from the metal surface via both multiphoton photoemission²³ and subsequent thermionic emission stay and accumulate at the photoexcited surface area. The resulting high density electron cloud creates a strong local electric field, commonly referred to as the space-charge effect. This transient space-charge field, if sufficiently large, will perturb a beam of charged particles (such as electrons). Real time and quantitative measurement of this perturbation to the charged particle permits accurate determination of time zero on the time scale primarily determined by dynamics of the transient field's buildup.

The time scale for the onset of space-charge field buildup is ultrafast and determined by multiphoton photoemission. To overcome the work function of ~ 4.26 eV at the Ag surface,²⁴ an electron at the Fermi level has to absorb at least three photons to escape. The kinetic energy of this photoexcited electron is 10 eV, equal to the 5.5 eV Fermi energy²⁵ plus the triple-photon energy, with a corresponding velocity of 1.9 nm/fs. The skin depth for three-photon absorption for Ag at 790 nm wavelength is unknown and we will use the value of ~ 11.4 nm²⁶ for single-photon absorption to estimate the field buildup time, since the skin depth should be much shorter for three-photon absorption due to its nonlinear nature. Given that the mean free path of photoelectrons is ~ 10 nm at a few eV above E_F ²⁷ (comparable to the

skin depth), the majority of photoelectrons will escape without suffering any collisions. Under this nearly ballistic transport condition, the average electron escape time would be ~ 10 fs. During this time, the photoelectrons can move only ~ 3 nm, since the velocity of a photoexcited electron drops from 1.9 to 0.3 nm/fs (0.24 eV kinetic energy) after escaping the Ag surface. These photoelectrons are spatially squeezed by more than a factor of 6 compared to inside of the Ag surface and accumulate as lone charges outside the Ag metal without any positive ion cores to balance them. As a result, a significant space-charge field could be created immediately after the multiphoton photoemission. Since the time scale of ~ 10 fs for this multiphoton photoemission is essentially instantaneous, the onset of this field, or equivalently the recorded onset of the perturbation of the charged particle beam, defines the time zero.

III. EXPERIMENTAL DESIGN AND RESULTS

The time zero measurement was carried out *in situ* on the femtosecond electron diffraction apparatus⁶ developed for the study of ultrafast structural dynamics in solids. The FED apparatus consists of four major components: an amplified femtosecond laser system, a femtosecond pulsed electron gun, a diffraction imaging system, and a streak camera. In a typical FED experiment, sub-50 fs optical pulses centered at 790 nm wavelength from the amplified Ti:sapphire laser system are used to initiate the structural dynamics. The structural changes are measured by taking snapshots of the diffraction patterns with fs probe electron pulses (60 keV) at different delay times. The digital images of diffraction patterns formed on the two-dimensional single-electron detector are captured using a charge coupled device camera with a spatial resolution of $33 \mu\text{m}$ per pixel and stored in a computer for subsequent analysis.

To avoid any potential walkoff, the time zero measurement was conducted in nearly identical experimental conditions as used in the FED, with the same electron ($\sim 300 \mu\text{m}$) and laser (~ 1 mm) beam sizes and the same beam crossing angle of less than 10° . After spatially overlapping the pump laser and probe electron beams with a pinhole, a silver needle mounted at the far end of the sample holder was brought into the interaction region to form a shadow image by blocking part of the *e*-beam. Shadow images both with and without the pump laser were then recorded at different time delays. To minimize the effect of pulse-to-pulse fluctuations in the electron beam intensity and beam pointing jitters, each image was averaged 500 shots. The intensities of pump laser and probe electron pulses could be adjusted continuously using two separate half wave plates in each optical arm.

Typical shadow images as a function of pump-probe delay times are shown in Fig. 1. They were recorded with 0.5 s integration time containing 500 pulses per image and using the excitation laser fluence of $30.6 \text{ mJ}/\text{cm}^2$. The average number of electrons per pulse was ~ 500 , with the corresponding temporal width less than 350 fs as measured by the streak camera.⁶ From these images, it is clearly seen that after the fs laser excitation the initial needle shadow started

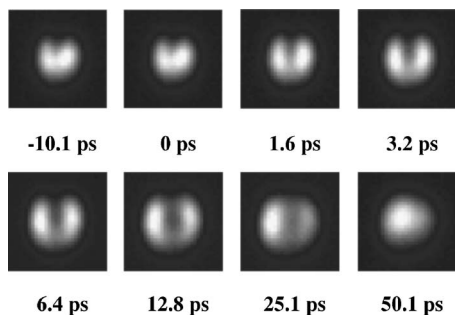


FIG. 1. Temporal evolution of electron shadow images of the silver needle. Each image was recorded using fs electron pulse containing an average of 500 electrons per pulse with 0.5 s integration time. The image size is 30×30 pixels and each square pixel corresponds to a dimension of $\sim 33 \times 33 \mu\text{m}^2$. The excitation laser fluence was 30.6 mJ/cm^2 and the corresponding time delays are shown at the bottom of each image.

to expand in two dimensions, predominantly along the vertical direction. This indicates that the space-charge cloud builds up mostly in the forward direction along the needle tip and expels high energy electrons in the e -beam via Coulomb repulsion. The expelled electrons, after gaining excess lateral kinetic energy, stroked the outer region, which is clearly shown as the concurrent expansion of the electron beam recorded in these images. This two dimensional expansion became progressively stronger initially as delay time increased. Then the shadow started to fade out at about 25 ps after excitation, with the simultaneous contraction of the electron beam size back to its original shape. The whole process persisted more than a few hundred ps.

The time zero point was determined by the quantitative evaluation of the temporal evolution of these shadow images. At each time delay, the change of image was calculated by summing the square of the intensity difference (SSD) in each corresponding pixel between two images recorded with and without pump laser. The temporal evolution of SSD curves measured at several different excitation laser fluences are displayed in Fig. 2. A few features are immediately noticeable. Clearly, a laser fluence larger than a threshold, which is about 10 mJ/cm^2 in the current experiment, is required to significantly change the SSD value. This threshold is directly associated with the requirement of a minimum number of emitted electrons to produce a sufficient space-charge field for detectable perturbation of the e -beam. Apparently, its actual value depends critically on several experimental parameters, such as electron beam size and energy, the shape, texture and material of the needle, the alignment of beams with the needle, and the spatial resolution of the imaging system. Additionally, the leading edge and the rising time of these curves do not show any significant dependence on the laser fluence within the range of $10\text{--}30 \text{ mJ/cm}^2$. This observation is consistent with the model's assumption that the transient field is created by electrons ejected via both multiphoton and thermionic emission, since neither dynamics was expected to undergo any significant changes within the applied excitation laser fluence.

The turning point of the SSD curve, defined here as the time zero measured by the ultrafast shadow imaging, was determined as the intersection point of two linear fittings of

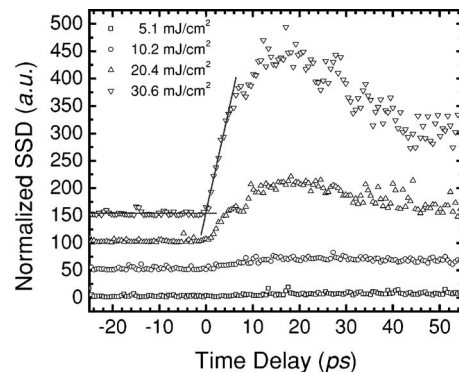


FIG. 2. Temporal evolution of the SSD curves at different excitation laser fluences. The time step is ~ 530 fs. Positive time delays correspond to the electron pulses arriving after excitation laser pulses. The time zero is defined by the crossing point of two linear fittings, one for the background (horizontal) before laser excitation and the other for the rising edge, shown in the SSD curve at fluence of 30.6 mJ/cm^2 .

the curve, one for the background before photoexcitation and the other for the rising edge. The typical uncertainty of the time zero point is less than 600 fs, which is calculated by the convolution of the errors in two linear fittings using standard error propagation rules.²⁸

The rising time of the SSD curve (τ_{tz}) reflects the dynamics of the electric field buildup and its interaction with the electron beam. It also sets the upper limit of the accuracy in the time zero measurement. Its value is determined by the convolution of the pump laser ($\tau_{\text{pump}}=50$ fs) and probe electron ($\tau_{\text{probe}} \approx 350$ fs) pulse widths, the effective buildup time of the transient electric field (τ_E) as seen by the probe electron beam, and the temporal degradation (τ_{mismatch}) due to the finite interaction volume. The magnitude of τ_{mismatch} in a typical experiment is estimated to be ~ 0.5 ps,²⁹ using the values of 1 mm for pump laser beam diameter, a probe e -beam size of $300 \mu\text{m}$, an effective needle diameter of $\sim 150 \mu\text{m}$ in the interaction region, and a 10° crossing angle of electron and laser beams. Considering that τ_{mismatch} is much smaller than the effective value of τ_{tz} at 4.8 ± 0.4 ps, which was obtained by fitting the rising edge in the SSD curve with a single exponential function, we may approximate τ_E as essentially the same as τ_{tz} . Assuming the transient electric field reaches its maximum strength instantaneously after the completion of electron emission, the shortest τ_E achievable would be the electron-phonon thermalization time ($\sim 1\text{--}2$ ps in noble metals). This is because the thermionic electron emission is nearly completely quenched after the electrons have transferred their energy to the lattice. Apparently, reducing the electron beam size to a dimension less than the laser-excited needle area ($\sim 150 \mu\text{m}$) will reduce τ_E to this ultimate value. Conversely, a larger size electron beam will increase τ_E . Such an effect has been observed with a defocused electron beam of ~ 2 mm in diameter, where τ_E as large as 50 ps was observed.

To evaluate the effects of set-to-set fluctuation and long-term drift of the FED apparatus on the time zero measurement, five sets of SSD curves were recorded in a 3 h time period. These sets were taken in identical experimental conditions by simply blocking the laser beams between each set.

The excitation laser fluence was 31 mJ/cm^2 and the e -beam averaged 650 electrons/pulse. The time zero points for each of these curves were first extracted following the procedure described above. Then the averaged time zero position and the corresponding uncertainty were calculated according to the laws of error propagation²⁸ by assuming each set was statistically independent of the others. The uncertainty (1 standard deviation) for the averaged time zero measurement is less than 700 fs.

Ideally, the true time zero could be extracted from the temporal evolution of the SSD curve by using a proper deconvolution scheme, provided that the spatial and temporal functional form of the transient space-charge field is known. However, in contrast to the conventional ultrafast optical pump-probe experiments where the transient commonly exhibits an exponential function of delay time, the actual function form for the transient field buildup is unknown. In addition, it is apparent that this function will not be uniquely defined since it relies on many factors such as the texture and geometry of the needle and also the alignment of the beams and the needle, which could be changed from experiment to experiment. All these factors complicate the determination of actual time zero using a conventional deconvolution approach. In contrast, the approach using the intersection of two linear fits outlined above can provide a quick and reliable reference point for the true time zero with a high precision of 700 fs. The true time zero should be 200–300 fs after this intersection point, corresponding to one third to one half of the temporal scale of convolution resulting from finite electron pulse ($<350 \text{ fs}$) and velocity mismatch ($\sim 500 \text{ fs}$). Nonetheless, this shift is within the reported uncertainty of 700 fs. In addition, it is expected that this systematic deviation should be a fixed number for the given experimental conditions and will not alter the $\sim 700 \text{ fs}$ precision.

ACKNOWLEDGMENTS

The authors would like to thank Dr. Pedro Schlottmann for helpful discussions and carefully reading the manuscript. This work was supported by the Florida State University and the National Science Foundation by Grant No. DMR-0305519.

- ¹J. C. Williamson, J. Cao, H. Ihee, H. Frey, and A. H. Zewail, *Nature* (London) **386**, 159 (1997).
- ²J. C. Williamson, PhD thesis, California Institute of Technology, Pasadena, CA, 1997.
- ³J. Cao, H. Ihee, and A. H. Zewail, *Proc. Natl. Acad. Sci. U.S.A.* **96**, 338 (1999).
- ⁴H. Ihee, V. A. Lobastov, U. M. Gomez, B. M. Goodson, R. Srinivasan, C. Y. Ruan, and A. H. Zewail, *Science* **291**, 458 (2001).
- ⁵R. Srinivasan, V. A. Lobastov, C. Y. Ruan, and A. H. Zewail, *Helv. Chim. Acta* **86**, 1763 (2003).
- ⁶J. Cao, Z. Hao, H. Park, C. Tao, D. Kau, and L. Blaszczyk, *Appl. Phys. Lett.* **83**, 1044 (2003).
- ⁷B. J. Siwick, J. R. Dwyer, R. E. Jordan, and R. J. D. Miller, *Science* **302**, 1382 (2003).
- ⁸C. Y. Ruan, V. A. Lobastov, F. Vigliotti, S. Y. Chen, and A. H. Zewail, *Science* **304**, 80 (2004).
- ⁹R. Srinivasan, J. S. Feenstra, S. T. Park, S. J. Xu, and A. H. Zewail, *Science* **307**, 558 (2005).
- ¹⁰H. Park, S. Nie, X. Wang, R. Clinite, and J. Cao, *J. Phys. Chem. B* (in press).
- ¹¹H. Park, X. Wang, S. Nie, R. Clinite, and J. Cao, *Solid State Commun.* (in press).
- ¹²R. R. Freeman, T. J. McIlrath, P. H. Bucksbaum, and M. Bashkansky, *Phys. Rev. Lett.* **57**, 3156 (1986).
- ¹³P. H. Bucksbaum, M. Bashkansky, and T. J. McIlrath, *Phys. Rev. Lett.* **58**, 349 (1987).
- ¹⁴C. I. Moore, J. P. Knauer, and D. D. Meyerhofer, *Phys. Rev. Lett.* **74**, 2439 (1995).
- ¹⁵R. W. Schoenlein, W. P. Leemans, A. H. Chin, P. Volfbeyn, T. E. Glover, P. Balling, M. Zolotarev, K. J. Kim, S. Chattopadhyay, and C. V. Shank, *Science* **274**, 236 (1996).
- ¹⁶T. J. Englert and E. A. Rinehart, *Phys. Rev. A* **28**, 1539 (1983).
- ¹⁷P. L. Kapitza and P. A. M. Dirac, *Proc. Cambridge Philos. Soc.* **29**, 297 (1933).
- ¹⁸P. H. Bucksbaum, D. W. Schumacher, and M. Bashkansky, *Phys. Rev. Lett.* **61**, 1182 (1988).
- ¹⁹See for example, *Ultrashort Laser Pulses: Generation and Applications*, edited by W. Kaiser (Springer, New York, 1993).
- ²⁰S. Williamson, G. Mourou, and J. C. M. Li, *Phys. Rev. Lett.* **52**, 2364 (1984).
- ²¹M. Dantus, S. B. Kim, J. C. Williamson, and A. H. Zewail, *J. Phys. Chem.* **98**, 2782 (1994).
- ²²J. Cao, H. Ihee, and A. H. Zewail, *Chem. Phys. Lett.* **290**, 1 (1998).
- ²³M. Aeschlimann, C. A. Schmuttenmaer, H. E. Elsayedali, R. J. D. Miller, J. Cao, Y. Gao, and D. A. Mantell, *J. Chem. Phys.* **102**, 8606 (1995).
- ²⁴H. B. Michaelson, *J. Appl. Phys.* **48**, 4729 (1977).
- ²⁵N. W. Ashcroft and N. D. Mermin, *Solid State Physics* (Saunders College Press, Philadelphia, 1976).
- ²⁶*Handbook of Optical Constants of Solids*, edited by E. D. Palik (Academic, Orlando, FL, 1985).
- ²⁷J. Cao, Y. Gao, H. E. Elsayed-Ali, R. J. D. Miller, and D. A. Mantell, *Phys. Rev. B* **58**, 10948 (1998).
- ²⁸P. R. Bevington and D. K. Robinson, *Data Reduction and Error Analysis for the Physical Sciences*, 3rd ed. (McGraw-Hill, New York, 2003).
- ²⁹J. C. Williamson and A. H. Zewail, *Chem. Phys. Lett.* **209**, 10 (1993).